

# Dpp signaling promotes the cuboidal-to-columnar shape transition of *Drosophila* wing disc epithelia by regulating Rho1

Thomas J. Widmann and Christian Dahmann\*

Max Planck Institute of Molecular Cell Biology and Genetics, Pfotenhauerstr. 108, 01307 Dresden, Germany

\*Author for correspondence (e-mail: dahmann@mpi-cbg.de)

Accepted 7 January 2009

Journal of Cell Science 122, 1362-1373 Published by The Company of Biologists 2009  
doi:10.1242/jcs.044271

## Summary

Morphogenesis is largely driven by changes in the shape of individual cells. However, how cell shape is regulated in developing animals is not well understood. Here, we show that the onset of TGF $\beta$ /Dpp signaling activity correlates with the transition from cuboidal to columnar cell shape in developing *Drosophila melanogaster* wing disc epithelia. Dpp signaling is necessary for maintaining this elongated columnar cell shape and overactivation of the Dpp signaling pathway results in precocious cell elongation. Moreover, we provide evidence that Dpp signaling controls the subcellular distribution of the activities of the small GTPase Rho1 and the regulatory light chain of non-muscle myosin II (MRLC). Alteration of Rho1 or MRLC activity has a profound effect on apical-basal cell length.

Finally, we demonstrate that a decrease in Rho1 or MRLC activity rescues the shortening of cells with compromised Dpp signaling. Our results identify a cell-autonomous role for Dpp signaling in promoting and maintaining the elongated columnar shape of wing disc cells and suggest that Dpp signaling acts by regulating Rho1 and MRLC.

Supplementary material available online at  
<http://jcs.biologists.org/cgi/content/full/122/9/1362/DC1>

Key words: *Drosophila*, Wing imaginal disc, Cell shape, Cell extrusion, Dpp, Tkv, Brk, Rho1, RhoGEF2, Myosin II

## Introduction

Cell growth, cell fate specification and morphogenesis are processes important for animal development. Secreted signaling molecules and their downstream signal transduction pathways have long been known to specify position-specific cell fate and to promote growth. However, less is known about how morphogenesis is regulated and how cell fate specification, growth and morphogenesis are orchestrated during animal development.

Morphogenesis of tissues is largely driven by changes in the shape of individual cells. The shape of cells depends mainly on the cytoskeleton and its associated proteins. One important class of regulators of actin-dependent change in cell shape is the Rho family of small GTPases (reviewed by Jaffe and Hall, 2005; Van Aelst and Symons, 2002). Rho (RhoA in vertebrates and Rho1 in *Drosophila*) can be activated by guanine nucleotide exchange factors (Rho-GEFs), which catalyze the exchange of GDP for GTP on Rho. Activated Rho-GTP interacts with several effectors, including the formin-homology-domain-containing protein Diaphanous (Dia), which promotes polymerization of actin filaments, and Rho-kinase (Rok) (reviewed by Ridley, 2006). One important substrate of Rok is the regulatory light chain of non-muscle myosin II (MRLC, encoded by *spaghetti squash*, *sqh*). Phosphorylation of MRLC induces activation of non-muscle myosin II (myosin II), and thereby promotes actin-myosin contraction (Amano et al., 1996). Rho1 signaling and myosin II are required for a variety of developmental processes, including apical constriction of epithelial cells during vertebrate neural tube formation, tubular morphogenesis, morphogenetic furrow progression and ventral furrow formation in *Drosophila* (Brodu and Casanova, 2006; Corrigan et al., 2007; Dawes-Hoang et al., 2005; Escudero et al.,

2007; Fox and Peifer, 2007; Kolsch et al., 2007; Nikolaidou and Barrett, 2004; Simoes et al., 2006; Wei et al., 2001), as well as cell rearrangements in the plane of the epithelium (Bertet et al., 2004; Escudero et al., 2007).

*Drosophila melanogaster* wing imaginal discs (wing discs) provide a model system in which to analyze cell fate specification, growth and epithelial morphogenesis. Wing discs are single-layered epithelia arranged in a sac-like structure that are fated to give rise to the adult wing blade and parts of the body wall (Fig. 1A-E) (Auerbach, 1936; Cohen, 1993). The morphology of the wing disc epithelium is developmentally regulated. During the first and early second instar larval stage, all cells are cuboidal. During the late second and early third instar larval stage however, cells on one side of this epithelial sac flatten and become squamous. Cells on the other side elongate and become highly columnar and pseudostratified (Ursprung, 1972; McClure and Schubiger, 2005). The transition from cuboidal to columnar cell shape might allow the accommodation of the exponentially increasing number of cells within the columnar epithelium during larval development. During pupal stage, cells regain a more cuboidal shape, which might help to extend the surface area of the developing wing to its final size (Fristrom and Fristrom, 1993). The signaling pathways and their cytoskeletal effectors that promote the transitions between cuboidal and columnar cell shape are not known.

Cell fate specification of the columnar cells of the wing disc pouch, the region that gives rise to the adult wing blade, requires signaling downstream of the Decapentaplegic (Dpp) signaling molecule, a member of the Transforming growth factor  $\beta$  (TGF $\beta$ ) superfamily (reviewed by Affolter and Basler, 2007). Dpp forms a protein gradient along the anteroposterior axis, with peak levels in the center of the

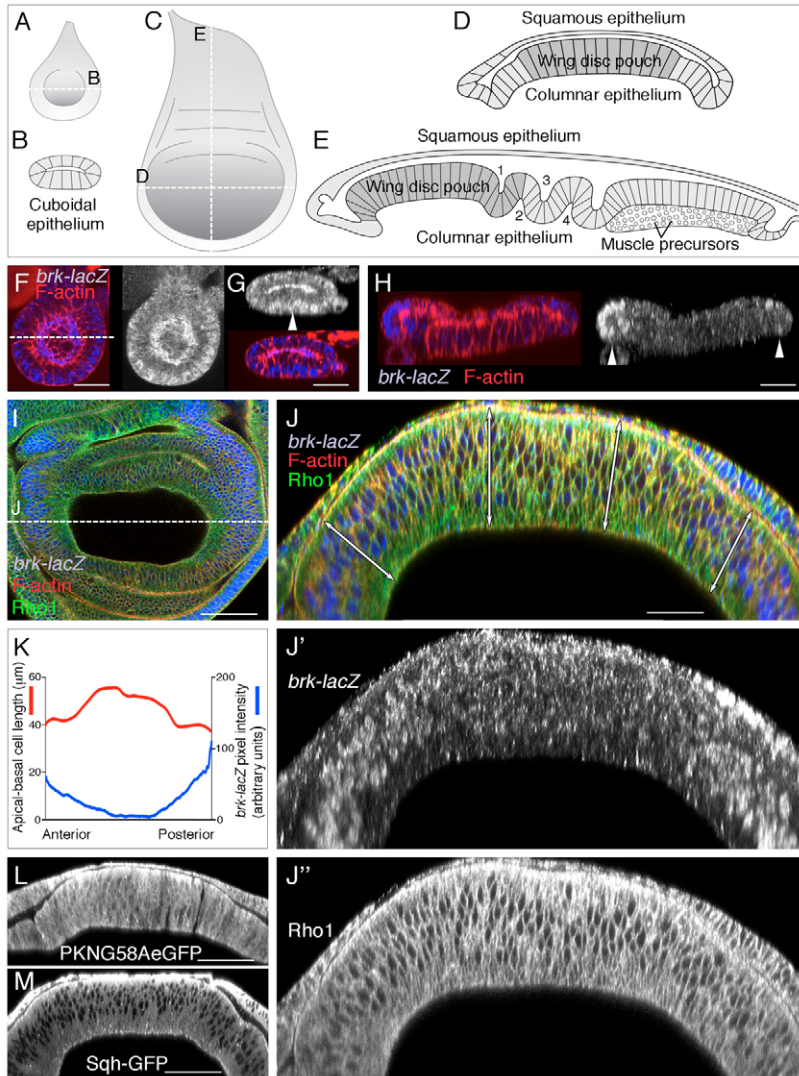


**Fig. 1.** Dpp signal transduction activity correlates with apical-basal cell length in wing discs. (A-E) Schemes of *x-y* (A,C) and cross section *x-z* (B,D,E) views of early-second instar (A,B) and late third instar (C-E) wing discs. The wing disc pouch is shaded in grey. Numbers in E refer to folds. Schemes are not to scale. (F-H) *x-y* (F) and *x-z* (G,H) views of wing discs from larvae  $48 \pm 3$  hours (F,G) and  $60 \pm 3$  hours (H) after egg lay, stained as indicated. *brk-lacZ* activity is detectable in most cells of wing discs at 48 hours, but restricted to peripheral cells at 60 hours after egg lay (arrowheads). (I,J) *x-y* (I) and *x-z* (J,J',J'') views of late third instar wing discs stained as indicated. Dpp signal transduction activity correlates with apical-basal cell length (double-sided arrows). Rho1 protein is enriched at the middle of the wing disc pouch. (K) Apical-basal cell length and pixel intensity of *brk-lacZ* as a function of the position along the anteroposterior axis for the image shown in J. (L,M) *x-z* views of late third instar wing discs stained as indicated. The Rho1 sensor (PKNG58AeGFP; *tub-GAL4 tubP-gal80<sup>ts</sup> UAS-PKNG58AeGFP* 24 hours after temperature shift to inducing conditions) and Sqh-GFP are enriched at the apicolateral side of the highly elongated cells in the middle of the wing disc pouch. Images in this figure are shown with the anterior to the left. In these and all subsequent *x-z* sections, apical of the columnar cells is to the top. Dotted lines indicate the position of *x-z* or *x-y* sections. Scale bars: 10  $\mu$ m (F-H); 50  $\mu$ m (I,L,M); 25  $\mu$ m (J).

wing disc and low levels at the periphery (Entchev et al., 2000; Teلمان and Cohen, 2000). Dpp signals through a conserved serine/threonine receptor kinase complex, including the type I receptor Thickveins (Tkv) (reviewed by Affolter and Basler, 2007). Dpp signal transduction results in the concentration-dependent activation of target genes and assigns position-specific cell fates within the wing disc (reviewed by Affolter and Basler, 2007).

Dpp signaling is also required for the growth of the wing. In flies carrying hypomorphic alleles of *dpp*, which severely reduce *dpp* expression in the wing disc, the adult wing is reduced to a small stump (Spencer et al., 1982; Zecca et al., 1995). Moreover, clones of cells mutant for *tkv* partly undergo apoptosis and fail to survive within the wing disc pouch (Adachi-Yamada et al., 1999; Adachi-Yamada and O'Connor, 2002; Burke and Basler, 1996; Martin-Castellanos and Edgar, 2002; Moreno et al., 2002). These findings have been taken as evidence that Dpp acts as a cell survival factor. Further analysis indicated that cells compete for Dpp and slow-growing cells are at a disadvantage to either compete for or transduce Dpp, and are thus eliminated from the epithelium, thereby maximizing tissue fitness (Moreno et al., 2002). More recent data showed that local loss of Dpp signaling in clones of cells mutant for *tkv* or *tkv* and *basket* (*bsk*, encodes c-Jun N-terminal kinase;

mutations of which suppress apoptosis induced in *tkv* mutant cells), undergo cytoskeletal rearrangements and are removed from the wing disc pouch by cell extrusion (Gibson and Perrimon, 2005; Shen and Dahmann, 2005a). These data indicate that Dpp signaling is required to maintain some aspect of the architecture of the wing disc pouch epithelium. However, cytoskeletal rearrangements and cell extrusion might not necessarily reflect a cell autonomous role for Dpp signaling in maintaining epithelial architecture, but might be consequences of the apposition of Dpp signaling cells and non-Dpp signaling cells at the clone border (Affolter and Basler, 2007). Moreover, it is not known in which developmental morphogenetic process Dpp normally acts, and whether Dpp signaling has also an instructive role in determining epithelial architecture. Finally, the cytoskeletal effectors mediating the morphogenetic function of Dpp remain elusive.

Here we show that Dpp signaling acts in a cell-autonomous and instructive manner to promote the transition from cuboidal to columnar epithelial cell shape during normal wing disc development. Moreover, we have identified Rho1 and myosin II as important mediators of Dpp signaling in the control of epithelial morphology. Our work also has more general implications for how cuboidal and columnar epithelial shape are determined.

## Results

### Dpp signal transduction activity correlates with apical-basal cell length in wing discs

During the late second and early third instar larval stages, cuboidal cells on one side of wing discs elongate along their apical-basal axis to become highly columnar. To test whether Dpp signal transduction activity levels are altered during this cuboidal-to-columnar cell shape transition, we stained wing discs for *brk-lacZ*, a marker for cells with little or no Dpp signal transduction activity (Campbell and Tomlinson, 1999; Jazwinska et al., 1999; Minami et al., 1999), and for F-actin to visualize cell shape. Apical-basal cell length was analyzed in optical cross-sections (*x-z*) taken along the anteroposterior axis. In the early second instar larval stage, *brk-lacZ* activity was detectable in most, if not all cells (Fig. 1F,G). Twelve hours later, *brk-lacZ* activity was confined to the cells of the wing disc periphery. *brk-lacZ* activity was not detectable in the cuboidal cells that underwent squamous morphogenesis (Fig. 1H), consistent with a role of Dpp signaling in this process (McClure and Schubiger, 2005). Furthermore, the prospective wing disc pouch cells that began to elongate no longer displayed detectable *brk-lacZ* activity (Fig. 1H). In the late third instar larval stage, the level of *brk-lacZ* activity inversely correlated with apical-basal cell length (Fig. 1I-K). High *brk-lacZ* activity in the periphery of the wing disc correlated with short cells. Cells with decreasing levels of *brk-lacZ* were increasingly elongated. Cells in the middle of the pouch region, which displayed little or no *brk-lacZ* activity, were most elongated. Staining for the small GTPase Rho1 revealed, in addition, that apical-basal cell length correlated with the subcellular distribution of Rho1 (Fig. 1J). Rho1 staining generally revealed cell outlines; however, cells in the middle of the pouch region showed increased Rho1 staining at their apicolateral region. To assess the spatial distribution of Rho1 activity, we used a GFP-based probe that binds the active, GTP-bound form of Rho1 (Simoes et al., 2006). Activity of this Rho1 sensor was detected throughout the wing disc epithelium and showed a moderate increase at the basal side of the cells (Fig. 1L). Similarly to the distribution of Rho1 protein, Rho1 sensor activity was increased at the apicolateral side of elongated cells present in the center of the wing disc pouch, compared with the shorter cells located at the wing disc periphery (Fig. 1L). Likewise, the abundance of MRLC protein, as visualized by Sqh-GFP, was increased at the apicolateral side of the highly elongated cells in the middle of the wing disc pouch (Fig. 1M). Thus, our data show that during early larval development, cell elongation correlates with an increase in Dpp signal transduction activity. In late larval development, Dpp signal transduction activity correlates with an elongated cell shape and increased Rho1 activity and MRLC abundance at the apicolateral region of cells. These findings indicate an important role for Dpp signaling, Rho1 and myosin II in the control of developmentally regulated changes in cell shape that normally occur in wing discs.

### Severe reduction of Dpp signaling in *tkv<sup>Δ12</sup> bsk<sup>-</sup>* clones initially results in apical cell constriction and cell shortening and ultimately results in cell extrusion

We first tested whether Dpp signal transduction is required for maintaining the highly elongated shape of wing disc pouch cells. To this end, we analyzed the morphological consequences of removing Dpp signaling locally within this epithelium. We generated marked *tkv<sup>Δ12</sup> Df(2L)flp147E (bsk<sup>-</sup>; bsk<sup>-</sup> suppresses apoptosis induced in *tkv<sup>Δ12</sup>* cells)* mutant cell clones in the second instar larval stage. The morphology of these mutant cell clones was analyzed over time using

E-cadherin, a component of apicolateral adherens junctions and Fasciclin III (FasIII), a marker of lateral membranes (Woods et al., 1997). Control *bsk<sup>-</sup>* clones maintained an apparently normal morphology (supplementary material Fig. S1) and expression of *tkv* from a transgene reverted the aberrant morphology of *tkv<sup>Δ12</sup> bsk<sup>-</sup>* mutant cells to wild type (supplementary material Fig. S1).

At 24 hours after clone induction, *tkv<sup>Δ12</sup> bsk<sup>-</sup>* mutant cells were apically constricted and shortened along their apical-basal axes compared with neighboring control cells (Fig. 2A-D). At 36-60 hours after clone induction, mutant cells had shortened further and were part of a deep epithelial invagination (Fig. 2E; supplementary material Movies 1 and 2). Control cells and *tkv<sup>Δ12</sup> bsk<sup>-</sup>* cells were facing the basal lamina component collagen IV, as visualized by *viking-GFP* (Fig. 2E). Adjacent control cells were part of the apical portion of the invagination. The lateral side of mutant cells, as revealed by FasIII, was positioned radially in the clone, pointing from the center of the clone towards the clone edges. PSβ-integrin, which in wild-type is mainly found at the basal side of cells (Fristrom et al., 1993), was enriched at the interface between mutant and control cells (supplementary material Fig. S1), indicating that the mutant and wild-type cells were apposed with their basal sides forming a basal indentation. E-cadherin, as well as Crumbs (Crb) and Discs large (Dlg), which are components of the subapical region and septate junctions, respectively (reviewed by Knust and Bossinger, 2002), were detected in the mutant cells (Fig. 2E,F; supplementary material Fig. S1 and our unpublished data), indicating that these cells had normal apical-basal polarity. At 60 hours, the number of *tkv<sup>Δ12</sup> bsk<sup>-</sup>* clones was reduced compared with *bsk<sup>-</sup>* control clones generated at the same time (our unpublished data), indicating that some *tkv<sup>Δ12</sup> bsk<sup>-</sup>* clones had already been lost from the epithelium, as reported previously (Gibson and Perrimon, 2005; Shen and Dahmann, 2005a). In a few clones, which were analyzed 60 hours after induction, we found that E-cadherin-based junctional contact between *tkv<sup>Δ12</sup> bsk<sup>-</sup>* cells and neighboring control cells was disrupted (Fig. 2G). Mutant cells were confined to the basal portion of the epithelium (Fig. 2G). These extruded mutant clones had an internal lumen and displayed E-cadherin at their apicolateral side (Fig. 2G). We also identified *tkv<sup>Δ12</sup> bsk<sup>-</sup>* clones apparently lacking an internal lumen, as visualized by FasIII, which was maintained (Fig. 2H,I). In these very late mutant clones, E-cadherin, Dlg and Crb were no longer concentrated at a particular site within the cell (Fig. 2H,I; supplementary material Fig. S1 and our unpublished data), indicating that mutant cells had lost part of their epithelial character. Induction of Snail and Twist, two transcription factors required for epithelial-to-mesenchymal transition (reviewed by Leptin, 2005), was not detected in these cells (supplementary material Fig. S1 and our unpublished data). Mutant cells displayed long actin-rich protrusions that were not observed in control cells (supplementary material Fig. S1) and were surrounded by collagen IV, as visualized by *viking-GFP* (Fig. 2H,I). This suggests that mutant cells are surrounded by basal lamina and then released from the epithelium without major disruption of the basal lamina. We did not detect remnants of CD8-GFP-labelled mutant cells within neighboring control cells (Fig. 2), as previously reported for cells eliminated by cell competition (Li and Baker, 2007). Aberrant cellular morphology of *tkv<sup>Δ12</sup> bsk<sup>-</sup>* clones was also observed outside the wing disc pouch, although with lower penetrance. Of the *tkv<sup>Δ12</sup> bsk<sup>-</sup>* clones located in the prospective hinge region, 23% ( $n=786$  clones scored in 75 wing discs) displayed epithelial invaginations. We conclude that Dpp signal

transduction is required to maintain the elongated shape of cells within the pouch and the prospective hinge region of wing discs.

Cells in *brk<sup>XH</sup> mad<sup>-</sup>* clones display a normal apical-basal length and do not extrude

Binding of Dpp to its receptor complex results in increased levels of the phosphorylated SMAD-related transcription factor Mothers against dpp (pMad), which, in turn, inhibits the transcriptional

repressor protein Brk and thereby induces target gene expression (reviewed by Affolter and Basler, 2007). Similarly to *tkv<sup>a12</sup> bsk<sup>-</sup>* mutant clones, *mad<sup>-</sup> bsk<sup>-</sup>* mutant clones are extruded from the wing disc pouch epithelium (Gibson and Perrimon, 2005; Shen and Dahmann, 2005a), indicating that Mad is required to maintain normal cell shape. To test whether Dpp signaling maintains cell shape through Mad-dependent repression of Brk, we generated *brk<sup>XH</sup> mad<sup>-</sup>* mutant clones. *brk<sup>XH</sup> mad<sup>-</sup>* mutant clones were recovered at a high frequency in the wing disc pouch (93% compared with control sibling clones,  $n=101$ ). As shown in Fig. 2J,K, apical-basal length appeared normal in *brk<sup>XH</sup> mad<sup>-</sup>* cells. We conclude that Dpp signaling maintains cell shape by Mad-dependent repression of Brk and hence transcriptional regulation of target genes.

A cell-autonomous role for Dpp signaling in maintaining the highly elongated shape of wing disc pouch cells

The apical constriction and invagination of cells in *tkv<sup>a12</sup> bsk<sup>-</sup>* clones might suggest that the normal role of Dpp is to prevent these changes in cell shape and maintain a flat and highly elongated epithelial layer. However, wild-type cells surrounding the mutant clone might influence the shape of cells inside the clone. To determine the cell-autonomous morphogenetic functions of Dpp signaling, we inhibited Dpp signal transduction in a large region of the wing disc – the dorsal compartment – and analyzed cell morphology. The ventral compartment served as an internal control. Daughters against dpp (*Dad*) is a potent inhibitor of Dpp signal transduction (Tsuneizumi et al., 1997). Coexpression of *Dad* and the baculovirus protein p35, an inhibitor of caspases (Hay et al., 1994) to suppress apoptosis, in clones of cells resulted in morphological changes that were similar to those observed in the *tkv<sup>a12</sup> bsk<sup>-</sup>* mutant clones (supplementary material Fig. S2). Time-controlled coexpression in the dorsal compartment of *Dad* and p35, using a temperature-inducible GAL4-UAS system (TARGET) (McGuire et al., 2003) (see Materials and Methods), strongly reduced pMad staining, a readout of the level of Dpp signal transduction (Tanimoto et al., 2000), throughout the dorsal compartment (supplementary material Fig. S2). Eight hours after temperature shift to induce *Dad* and p35, we detected no obvious difference in the shape of dorsal and ventral cells (Fig. 3A). After 48 hours, an apical invagination had formed close to the dorsal-ventral compartment boundary and, notably, cells throughout the dorsal compartment were significantly shorter along their apical-basal axis (Fig. 3B,I). After 56 hours, a deep apical invagination and a basal indentation, as revealed by the apposition of PS $\beta$ -integrin-stained adjacent dorsal and ventral cell membranes, had formed close to the dorsal-ventral compartment boundary (Fig. 3C,D), which was similar to what we observed at the borders of *tkv<sup>a12</sup> bsk<sup>-</sup>* clones. Notably, cells throughout the dorsal compartment had further shortened (Fig. 3C,I). The  $x$ - $z$  cross-sectional area of cells was reduced in dorsal cells compared with ventral cells to an extent expected if cell volume had remained unchanged (Fig. 3I), indicating that coexpression of *Dad* and p35 did not result in a change of cell volume but rather in cell shape. Dorsal cells displaying a reduced length were still part of the wing disc pouch, as shown by the folding of the epithelium (Fig. 3A-C) and the expression of Wingless (supplementary material Fig. S2), which marks the border of the pouch region (Azipiazu and Morata, 2000). Expression of p35 alone had no obvious effect on cell shape (data not shown). Moreover, expression of *tkv<sup>AGSK</sup>* in the dorsal compartment, which results in decreased Dpp signal transduction (Haerry et al., 1998), gave rise to comparable changes in cell shape

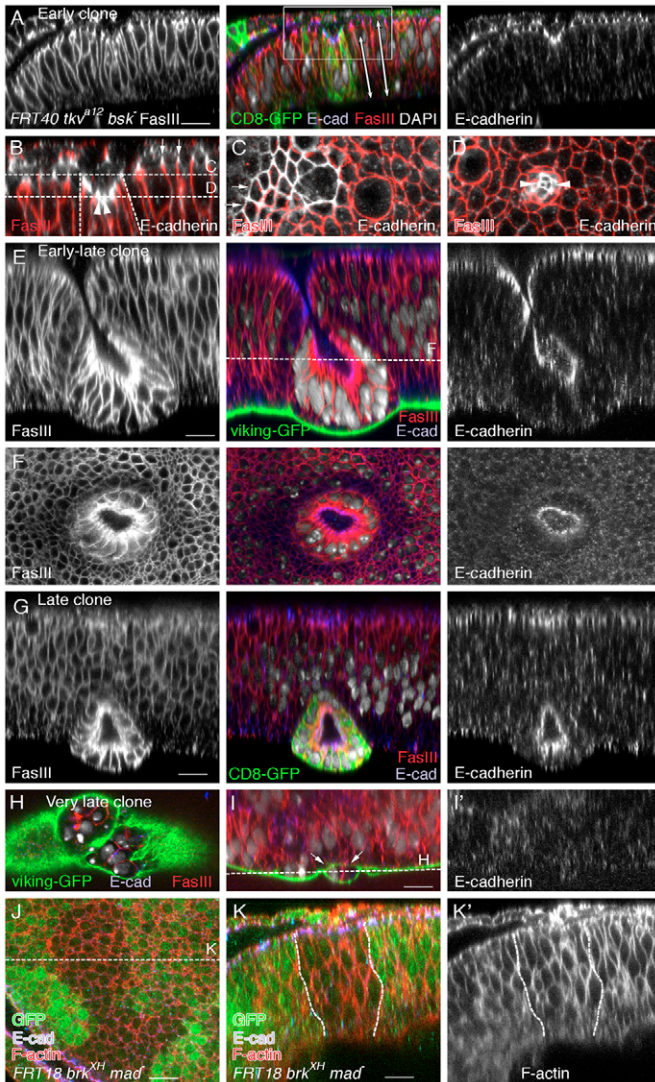
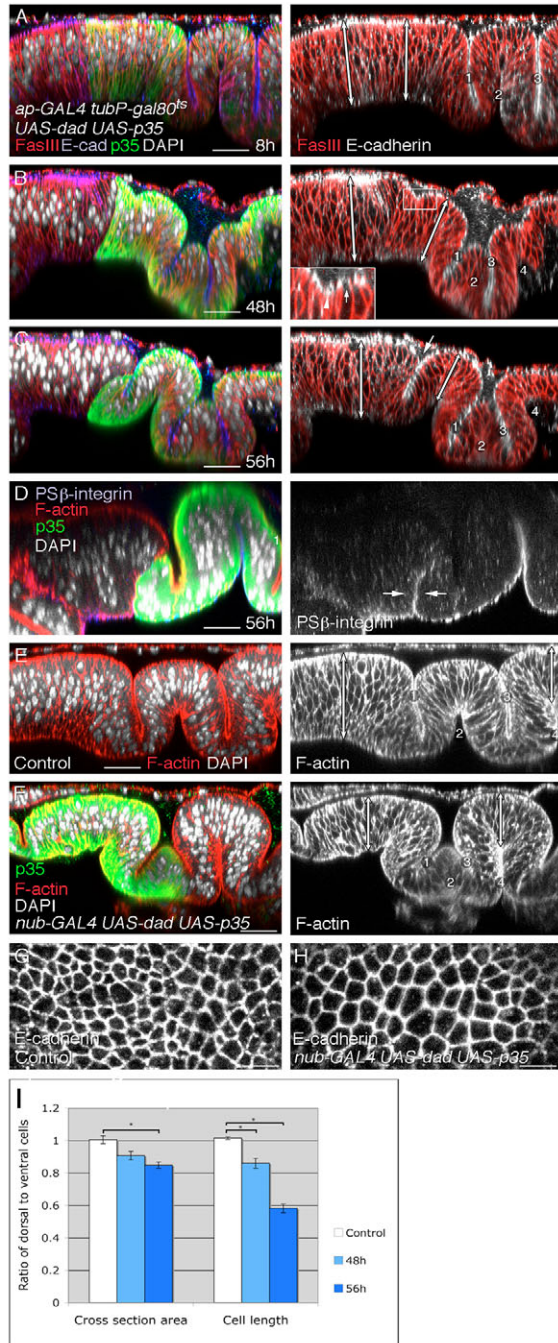


**Fig. 2.** Cells in *tkv<sup>a12</sup> bsk<sup>-</sup>* clones are apically constricted and short, and are extruded from the epithelium. (A-I) Clones of *tkv<sup>a12</sup> bsk<sup>-</sup>* cells, identified in A and G by the presence of CD8-GFP, were induced at the second instar larval stage and stained as indicated 24 hours (A-D) or 48-60 (E-I) hours later. (A)  $x$ - $z$  view. *tkv<sup>a12</sup> bsk<sup>-</sup>* cells are shorter along the apical-basal axis than control cells (double-sided arrows). (B) Magnified view of the boxed area in the middle panel of A. Vertical dotted lines isolate the clone. (C,D)  $x$ - $y$  sections of B. *tkv<sup>a12</sup> bsk<sup>-</sup>* cells are apically constricted (arrowheads) compared with control cells (arrows). (E)  $x$ - $z$  view. *tkv<sup>a12</sup> bsk<sup>-</sup>* cells are part of a deep epithelial fold. (F)  $x$ - $y$ -section of E. (G)  $x$ - $z$  view. *tkv<sup>a12</sup> bsk<sup>-</sup>* cells have lost contact with the zonula adherens of neighboring control cells and form cyst-like structures. (H)  $x$ - $y$  section. (I)  $x$ - $z$  view. E-cadherin is greatly reduced in mutant cells. Arrows indicate *tkv<sup>a12</sup> bsk<sup>-</sup>* cells surrounded by Viking-GFP. (J,K) Clones of *brk<sup>XH</sup> mad<sup>-</sup>* cells, marked by the absence of GFP (green), induced at the second instar larval stage and stained 60 hours later. (J)  $x$ - $y$  view. (K)  $x$ - $z$ -section of J. *brk<sup>XH</sup> mad<sup>-</sup>* cells display a normal apical-basal length. Scale bars: 10  $\mu$ m.



to those seen upon coexpression of Dad and p35 (data not shown). Finally, coexpression of Dad and p35 throughout the entire wing disc pouch resulted in shorter and apically wider cells throughout this area (Fig. 3E-H). Thus, the primary role of Dpp is not to prevent apical constriction of cells and epithelial invagination, but rather to maintain, in a cell-autonomous manner, the highly elongated columnar shape of wing disc pouch cells.

Dpp signaling is required for the apicolateral increase of Rho1 and myosin II activity

We next analyzed additional molecular markers in wing discs coexpressing Dad and p35 in cells of the dorsal compartment. FasIII and PS $\beta$ -integrin were not obviously changed in dorsal cells

**Fig. 3.** A cell-autonomous role for Dpp signaling in maintaining a highly elongated cell shape. (A-D) *x-z* sections of wing discs coexpressing Dad and p35 in the dorsal compartment at the indicated time after temperature shift to inducing conditions and stained as indicated. (A-C) Cells of the dorsal pouch region become shorter over time compared with the ventral control cells (double-sided arrows). (B) Epithelium forms an apical invagination a few cell rows into the dorsal compartment (inset). Cells in the apical invagination are apically constricted (arrowhead) compared with cells located more dorsally (arrow). (C) A deep epithelial invagination (arrow) formed at the dorsal-ventral compartment boundary. (D) A basal indentation containing PS $\beta$ -integrin formed (arrows). (E,F) *x-z* sections of control wing disc (E) and wing disc coexpressing Dad and p35 under the control of *nub-GAL4* in the wing disc pouch (F) stained as indicated. Cells coexpressing Dad and p35 are shorter along their apical-basal axis than pouch cells of the control (double-sided arrows on the left hand side). Prospective hinge cells, which do not display *nub-GAL4* activity, serve as an internal control (double-sided arrows to the right). The pouch region in F is smaller compared to the pouch region in E. Epithelial fold shown on the left in F corresponds to a normal ventral hinge fold. Numbers in A-F denote folds in the wing disc (compare with Fig. 1E). *x-z* sections in A-F and Figs 4-7 are taken approximately through the center of the wing disc perpendicular to the dorsal-ventral compartment boundary; dorsal is shown to the right. (G,H) *x-y* sections of the pouch region of control wing disc (G) and wing disc coexpressing Dad and p35 under control of *nub-GAL4* (H) stained for E-cadherin. Cells coexpressing Dad and p35 display an increased apical circumference compared to controls. (I) Quantifications of *x-z* cross-section area and apical-basal cell length. Ratios between dorsal and ventral cells in control wing discs (*UAS-dad UAS-p35*) and *ap-GAL4 tubP-gal80<sup>ts</sup> UAS-dad UAS-p35* wing discs 48 hours and 56 hours after temperature shift to inducing conditions are shown. Cells coexpressing Dad and p35 are significantly shorter and display a moderately reduced cross-section area compared with control cells. Means  $\pm$  s.e.m. are shown [ $n=9$  wing discs (control);  $n=7$  (48h);  $n=14$  (56h)]; \* $P<0.001$ . Scale bars: 20  $\mu$ m (A-F); 5  $\mu$ m (G,H).

compared with control ventral cells (Fig. 3A-D). Moesin, a member of the ezrin, radixin and moesin (ERM) family of proteins that are important for the anchoring of actin microfilaments to the cell cortex (reviewed by Polesello and Payre, 2004), was highly reduced at the apicolateral side of cells throughout the dorsal compartment, as in *tkv<sup>al2</sup> bsk<sup>-</sup>* clones (Fig. 4A; supplementary material Fig. S1). Furthermore, a dense apical network of microtubules, present in wild-type cells (Eaton et al., 1996) and absent in *tkv<sup>al2</sup> bsk<sup>-</sup>* clones (Gibson and Perrimon, 2005; Shen and Dahmann, 2005a), was highly reduced in dorsal cells (Fig. 4B). Moreover, staining for Rho1 protein and Rho1 sensor activity showed that both were greatly reduced on the apicolateral side of dorsal cells compared with control cells stained in the same experiment (Fig. 4C-E) (see Materials and Methods). Phosphorylated MRLC (P-MRLC), which is a measure of active myosin II and is normally enriched at the apicolateral membrane of elongated wing disc cells, was distributed uniformly throughout the dorsal cells (Fig. 4F). Thus, Dpp signal transduction is required cell autonomously to maintain apically localized moesin, the apical microtubule network and the high levels of Rho1 and myosin II activities at the apicolateral side of wing disc pouch cells.

Activation of Dpp signal transduction results in an apicolateral increase in Rho1 activity and precocious cell elongation

To test whether Dpp signal transduction is sufficient to promote cell elongation during early development, we expressed an activated form of the Dpp receptor Tkv, Tkv<sup>Q-D</sup> (Lecuit et al., 1996; Nellen et al., 1996), in dorsal cells and analyzed cell morphology in early and late third instar wing discs. Ventral and dorsal pouch cells of control early third instar wing discs displayed a similar apical-basal length (Fig. 5A,I). By contrast, dorsal pouch cells of early third instar discs expressing Tkv<sup>Q-D</sup> were ~1.4-fold longer along the

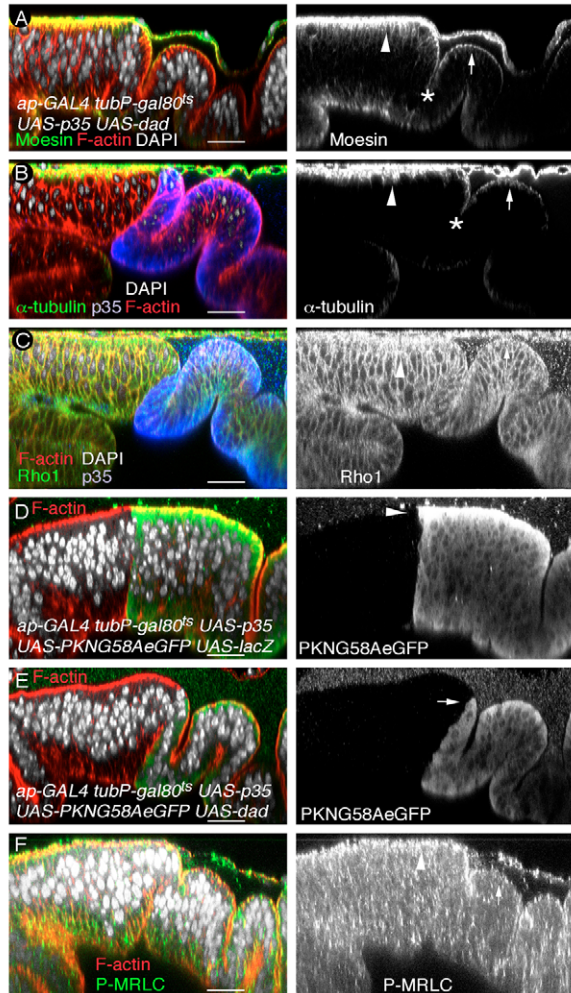


**Fig. 4.** Dpp signaling is required for elevated levels of Rho1 sensor activity at the apicolateral side of cells. (A–C,F) *x-z* sections of wing discs coexpressing Dad and p35 in the dorsal compartment 56 hours after temperature shift to inducing conditions and stained as indicated. (A) Apicolaterally localized moesin is reduced in dorsal cells (arrow) compared with ventral cells (arrowhead) and is strongly reduced in the apical invagination (asterisk). (B) The apical microtubule network is highly reduced in dorsal cells (arrows) compared with ventral cells (arrowhead) and is undetectable in cells located deep in the apical invagination (asterisk). (C) Apicolaterally localized Rho1 is reduced in dorsal cells (arrow) compared with ventral control cells (arrowhead). (D,E) *x-z* sections of wing discs coexpressing p35, PKNG58AeGFP (Rho sensor) and *lacZ* (D) or p35, PKNG58AeGFP and Dad (E) in the dorsal compartment 56 hours after temperature shift to inducing conditions, and stained as indicated. Rho sensor activity is reduced on the apicolateral side of Dad-expressing cells (arrow) compared with control *lacZ*-expressing cells (arrowhead). (F) Apicolaterally localized P-MRLC is reduced in dorsal cells (arrow) compared to ventral cells (arrowhead). Dorsal compartment is shown to the right in A–F. Scale bars: 20  $\mu$ m.

apical-basal axis compared with the ventral control cells (Fig. 5B,I). In contrast to the control cells, *Tkv<sup>Q-D</sup>*-expressing cells were pseudostratified (Fig. 5B). The apical cell circumference of *Tkv<sup>Q-D</sup>*-expressing cells was decreased compared with control cells (Fig. 5C). The shape of prospective dorsal hinge cells was not obviously altered (Fig. 5B). F-actin, moesin and FasIII were not obviously altered in *Tkv<sup>Q-D</sup>*-expressing cells (Fig. 5B,J; and our unpublished data). The abundance of Rho1 was similar at the lateral sides of control cells and *Tkv<sup>Q-D</sup>*-expressing cells ( $106.35 \pm 2.43$  and

$107.16 \pm 2.01$ , respectively; mean  $\pm$  s.e.m. of pixel intensities in arbitrary units). By contrast, Rho1 was enriched at the apicolateral side in *Tkv<sup>Q-D</sup>*-expressing cells compared with ventral control cells (Fig. 5D,J). Moreover, Rho1 sensor activity and MRLC abundance were also increased at the apicolateral side of *Tkv<sup>Q-D</sup>*-expressing cells (Fig. 5E–G,J). A moderate increase in Rho1 and MRLC abundance and Rho1 sensor activity was also observed at the basal side of the *Tkv<sup>Q-D</sup>*-expressing cells (Fig. 5D–G). In late third instar wing discs, dorsal pouch cells were moderately, but reproducibly, longer along their apical-basal axis compared with control ventral cells (Fig. 5H,I). We conclude that the activation of Dpp signal transduction is sufficient to induce an increase in Rho1 activity and MRLC abundance at the apicolateral and basal sides of cells, and to promote the elongation and apical narrowing of cells within the wing disc pouch during larval development.

#### Rho1 and myosin II affect apical-basal cell length

How does Dpp signaling control the apical-basal length of wing disc pouch cells? We have shown above that cell shortening, resulting from the reduction of Dpp signaling throughout the dorsal compartment, correlated with cell autonomous reductions of the apical microtubule network and of apicolaterally localized moesin, Rho1 and MRLC. Interfering with the apical microtubule network, through coexpression of the microtubule-severing protein katanin 60 and kinesin-like protein 1 (Klp1) (Goshima and Vale, 2003; McNally and Vale, 1993), had no immediate effect on the highly columnar cell shape (supplementary material Fig. S3). Moreover, consistent with a previous report (Speck et al., 2003), strong reduction of moesin levels by RNA interference (RNAi) resulted in the disintegration of the epithelium, and thus, specific effects on columnar cell shape could not be analyzed (supplementary material Fig. S4). By contrast, coexpression throughout the dorsal compartment of a dominant-negative form of Rho1, *Rho1<sup>N19</sup>* (Strutt et al., 1997), and p35, resulted in cells that were more highly elongated along the apical-basal axis compared with control ventral cells (Fig. 6A,G). Similarly, a strong reduction of Rho1 protein levels by RNAi resulted in more highly elongated cells (Fig. 6B,G).

To test whether Rho1 is sufficient to alter wing disc cell shape, we expressed an activated form of Rho1, *Rho1<sup>V14</sup>* (Lee et al., 2000). Expression of *Rho1<sup>V14</sup>* throughout the dorsal compartment resulted in shorter cells throughout this region, compared with control ventral cells (Fig. 6C,G). Dpp signaling activity, measured by expression of the Dpp target Spalt (Lecuit et al., 1996; Nellen et al., 1996), was not obviously altered (Fig. 6C), indicating that expression of *Rho1<sup>V14</sup>* does not alter cell shape by downregulating Dpp-signaling activity. Likewise, expression of *RhoGEF2*, a guanine nucleotide exchange factor activating Rho1 (Barrett et al., 1997; Hacker and Perrimon, 1998), gave rise to shorter cells (Fig. 6D,G). We conclude that Rho1 activity has a profound effect on the apical-basal length of wing disc cells.

Rho1 acts through several effectors, including Dia and myosin II (see Introduction). Severe reduction of Dia protein levels by RNAi had no detectable effect on apical-basal cell length (supplementary material Fig. S4). By contrast, RNAi-mediated reduction of MRLC resulted in more highly elongated cells (Fig. 6E,G), which was similar to results observed when Rho1 activity was decreased. Conversely, mutations in *mbs*, encoding a subunit of myosin light chain phosphatase, that lead to increased myosin II activity (Alessi et al., 1992; Hartshorne et al., 1998), or expression of an activated form of MRLC, *sqh<sup>E20E21</sup>* (Winter et al., 2001), gave rise to short cells (Figs 6F,G; supplementary material Fig. S5) (Mitonaka et al.,

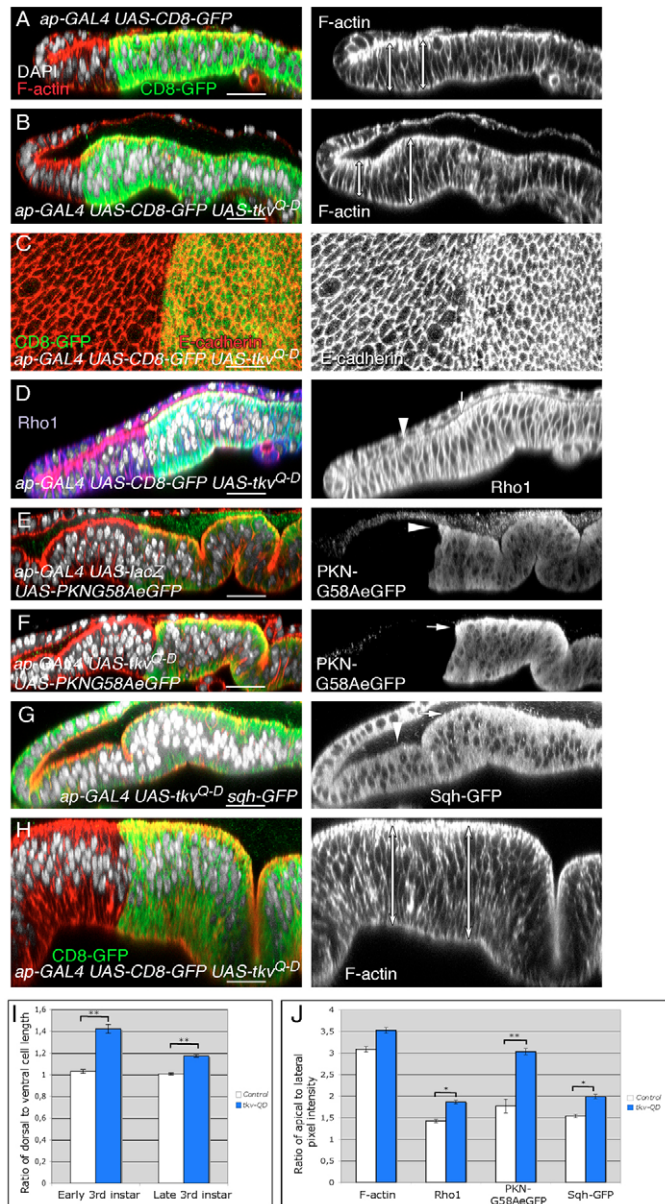


**Fig. 5.** Increased Dpp signaling results in elevated Rho1 sensor activity at the apicolateral side of cells and in precocious cell elongation. (A) *x-z* section of early third instar control wing disc expressing CD8-GFP under the control of *ap-GAL4* in the dorsal compartment and stained as indicated. Dorsal and ventral cells have a similar apical-basal cell length (double-sided arrows). (B-D) *x-z* sections (B,D) or a projection of *x-y* sections (C) of early third instar wing discs coexpressing *Tkiv<sup>Q-D</sup>* and CD8-GFP under the control of *ap-GAL4* stained as indicated. Cells within the presumed pouch region coexpressing *Tkiv<sup>Q-D</sup>* and CD8-GFP are pseudostratified and longer (double-sided arrows), are apically constricted and display increased Rho1 at their apicolateral sides (arrow) compared with control ventral cells (arrowhead). (E-G) *x-z* section of early third instar wing discs coexpressing *lacZ* and PKNG58AeGFP (Rho sensor) (E), *Tkiv<sup>Q-D</sup>* and PKNG58AeGFP (F) or *Tkiv<sup>Q-D</sup>* (G) under the control of *ap-GAL4* in the dorsal compartment and stained as indicated. In G, *Sqh-GFP* is, in addition, expressed under its own promoter to visualize MRLC. *Tkiv<sup>Q-D</sup>*-expressing cells display increased *Sqh-GFP* abundance and Rho sensor activity (arrows) compared with control cells (arrowheads). (H) *x-z* section of a late third instar wing disc coexpressing *Tkiv<sup>Q-D</sup>* and CD8-GFP under the control of *ap-GAL4* stained as indicated. Cells coexpressing *Tkiv<sup>Q-D</sup>* and CD8-GFP are moderately longer than control cells (double-sided arrows). (I) Ratio of apical-basal length between dorsal and ventral cells in control wing discs (*ap-GAL4, UAS-CD8-GFP*) and wing discs coexpressing CD8-GFP and *Tkiv<sup>Q-D</sup>* in the dorsal compartment (*ap-GAL4 UAS-CD8-GFP UAS-Tkiv<sup>Q-D</sup>*) of early third instar and late third instar larvae are shown. Means  $\pm$  s.e.m. are indicated ( $n=11$  wing discs (early, control);  $n=15$  (early, *Tkiv<sup>Q-D</sup>*);  $n=14$  (late, control);  $n=4$  (late, *Tkiv<sup>Q-D</sup>*);  $**P<0.001$ ). (J) Ratio of apical to lateral pixel intensities for F-actin, Rho1, PKNG58AeGFP and *Sqh-GFP* staining of ventral control cells and dorsal cells coexpressing CD8-GFP and *Tkiv<sup>Q-D</sup>*. Means  $\pm$  s.e.m. are indicated [ $n=14$  wing discs (F-actin);  $n=9$  (Rho1);  $n=5$  (PKNG58AeGFP, control);  $n=8$  (PKNG58AeGFP, *Tkiv<sup>Q-D</sup>*);  $n=8$  (*Sqh-GFP*)];  $*P<0.05$ ;  $**P<0.001$ . Scale bars: 20  $\mu\text{m}$  (A,B,D-H); 10  $\mu\text{m}$  (C).

apical-basal cell length (Fig. 7D), indicating that the suppression of cell shortening is specific. Dpp signal transduction was highly decreased in cells coexpressing *Rho1<sup>N19</sup>*, *Dad* and *p35*, as monitored by the expression of *Spalt* (Fig. 7A). We conclude that Dpp signal transduction regulates apical-basal cell length by regulation of a Rho1–myosin-II pathway.

## Discussion

Transitions between squamous, cuboidal and columnar epithelial cell shapes are common during animal development and contribute to the morphogenesis of complex tissue and organ shapes. Here, we demonstrate a cell-autonomous and instructive role for the Dpp-signaling pathway in promoting the cuboidal-to-columnar shape transition of larval wing disc pouch cells. Moreover, we describe a function for Rho1 and myosin II in the regulation of apical-basal cell length and provide evidence that Rho1 mediates the ability of Dpp to control epithelial morphology. A possible link between inappropriate cell shape and cell extrusion is discussed.

### Extrusion of cell clones with severely reduced Dpp signaling

We observed cell extrusion when Dpp signaling was locally reduced in *tkv<sup>Δ12</sup> bsk<sup>-</sup>* clones, but not when it was reduced throughout the dorsal compartment by expression of *Dad* (Fig. 8A,B). This indicates that cell extrusion is a consequence of the sharp boundary of Dpp signaling at the clone border. One of the first morphological consequences of the loss of Dpp signaling in *tkv<sup>Δ12</sup> bsk<sup>-</sup>* clones was the apical constriction of mutant cells and surrounding control cells (Fig. 2A–D). Apical constriction correlated with increased staining intensities of F-actin and P-MRLC, a marker for active non-muscle myosin II (Craig et al., 1983), at the apicolateral side of *tkv<sup>Δ12</sup> bsk<sup>-</sup>* and neighboring wild-type cells (supplementary material Fig. S1 and our unpublished data). The formation of a similar actin-myosin ring has been previously demonstrated during the extrusion of apoptotic

2007). These results suggest that Rho1 affects apical-basal cell length by regulating myosin II activity.

A decrease in Rho1 or myosin II activity rescues the shortening of cells with compromised Dpp signaling

To test whether Dpp signal transduction regulates apical-basal cell length through modulating a Rho1–myosin II pathway, we coexpressed several proteins together with *Dad* and *p35* throughout the dorsal compartment of wing discs and analyzed cellular morphology. Coexpression of GFP resulted in highly reduced apical-basal cell length compared with control ventral cells (Fig. 7D). By contrast, cells coexpressing *Rho1<sup>N19</sup>*, double-stranded RNA targeting *sqh*, or *Mbs<sup>N300</sup>*, an activated form of *Mbs* (Lee and Treisman, 2004), together with *Dad* and *p35*, displayed an apical-basal cell length comparable to that in the control ventral cells (Fig. 7A–D). Expression of *Mbs<sup>N300</sup>* in wild-type cells did not affect

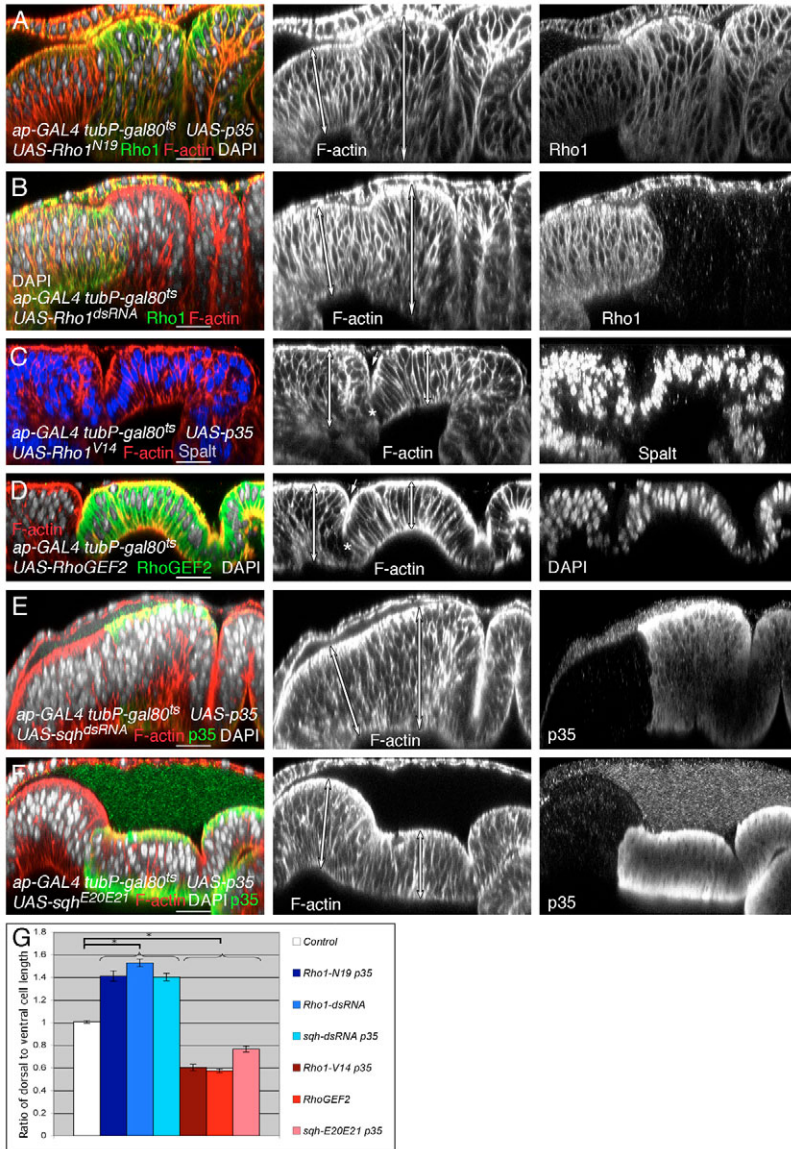


**Fig. 6.** Rho1 and myosin II affect apical-basal cell length. (A-F) *x-z* sections of late third instar wing discs expressing Rho1<sup>N19</sup> and p35 (A), double-stranded RNA targeting Rho1 (*Rho1<sup>dsRNA</sup>*) (B), Rho1<sup>V14</sup> and p35 (C), RhoGEF2 (D), *sqh<sup>dsRNA</sup>* and p35 (E) or *sqh<sup>E20E21</sup>* and p35 (F) in the dorsal compartment, 44 hours (A,B), 8 hours (C), 17 hours (D), 48 hours (E) or 56 hours (F) after temperature shift to inducing conditions and stained as indicated. (A,B) Cells expressing Rho1<sup>N19</sup> or *Rho1<sup>dsRNA</sup>* are more highly elongated along the apical-basal axis compared with control ventral cells (double-sided arrows). (C,D) Cells expressing Rho1<sup>V14</sup> or overexpressing RhoGEF2 are shorter than control cells (double-sided arrows) and tend to be packed more regularly. Cells at the interface between the Rho1<sup>V14</sup> or RhoGEF2 overexpression domain and control cells are even shorter (asterisk) and form an epithelial invagination (arrow). Cells expressing *sqh<sup>dsRNA</sup>* (E) are more highly elongated and cells expressing *sqh<sup>E20E21</sup>* (F) are shorter compared with control ventral cells (double-sided arrows). (G) The ratio of apical-basal length between dorsal and ventral cells of the experiments shown in A-F. Means  $\pm$  s.e.m. are depicted [ $n=14$  wing discs (control);  $n=14$  (*Rho1<sup>N19</sup>*, p35);  $n=5$  (*Rho1<sup>dsRNA</sup>*);  $n=11$  (*sqh<sup>dsRNA</sup>*, p35);  $n=13$  (*Rho1<sup>V14</sup>*, p35);  $n=10$  (*RhoGEF2*);  $n=6$  (*sqh<sup>E20E21</sup>*, p35)]; \* $P<0.001$ . Scale bars: 20  $\mu$ m.

cells, and it has been proposed that contraction of this ring squeezes cells out of the epithelium (Rosenblatt et al., 2001). It is currently unclear whether these increased staining intensities reflect an increase in the total amount of F-actin and P-MRLC in *tkv<sup>Δ12</sup> bsk<sup>-</sup>* mutant clones, or whether they are instead merely a consequence of the apical constriction of cells. Nevertheless, these findings are consistent with the view that contraction of an actin-myosin ring might contribute to the extrusion of *tkv<sup>Δ12</sup> bsk<sup>-</sup>* cells. Apical cell constriction was paralleled with cell shortening along the apical-basal axis. Based on our observation that reduction in Dpp signaling throughout the wing disc pouch resulted in apical-basal cell shortening, but not in apical cell constriction, we speculate that cell shortening, and thus the formation of an inappropriate cell shape, might be an initial event leading to the extrusion of *tkv<sup>Δ12</sup> bsk<sup>-</sup>* cells. If so, cell extrusion might not represent a specific response to eliminate slow-growing or apoptotic cells, but rather represents a general response to inappropriate cell function or morphology. In the wild type, cell extrusion might be instrumental in maximizing tissue fitness by removing cells with inappropriate function or morphology.

We also found that the basal membrane of *tkv<sup>Δ12</sup> bsk<sup>-</sup>* cells and neighboring control cells, identified by PSβ-integrin labeling, became apposed (supplementary material Fig. S1). As this led to a reduction in the lateral contact between mutant and neighboring control cells, this apposition might help to dislodge *tkv<sup>Δ12</sup> bsk<sup>-</sup>* cells from the remaining epithelium, and thereby, might aid the extrusion process. We also noted that extruded *tkv<sup>Δ12</sup> bsk<sup>-</sup>* cells displayed features reminiscent of epithelial-to-mesenchymal transition (EMT). In particular, a strong decrease in E-cadherin, a hallmark of EMT (reviewed by Thiery and Sleeman, 2006) and actin-rich processes were observed in extruded *tkv<sup>Δ12</sup> bsk<sup>-</sup>* cells. Interestingly, a role for Dpp/BMPs in preventing EMT has also been identified in vertebrates. Mouse BMP7, which is related to Dpp, for example, is required for counteracting EMT associated with renal fibrosis (reviewed by Zavadil and Bottinger, 2005). Decreased E-cadherin levels have also recently been reported following the extrusion of cells deficient for C-terminal Src kinase from *Drosophila* epithelia (Vidal et al., 2006), indicating that this might be a more common consequence of cell extrusion.

### A cell-autonomous function for Dpp signaling in controlling columnar cell shape

We observed reduced apical-basal cell length when Dpp signaling was severely reduced, either in clones or throughout the wing disc pouch; however, apical cell constriction, fold formation and cell extrusion were only detected by clonal reduction of Dpp signaling. Instead, cells were apically widened and did not extrude when Dpp signaling was reduced throughout the dorsal compartment. These experiments therefore allowed us to separate the effects of sharp

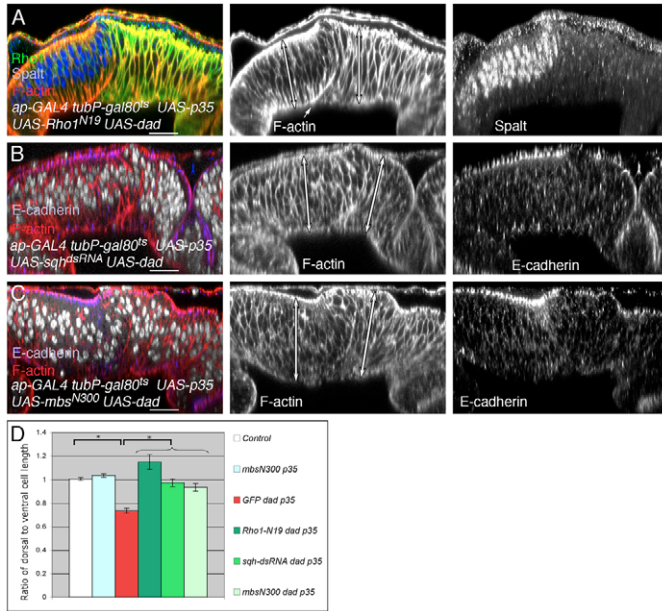
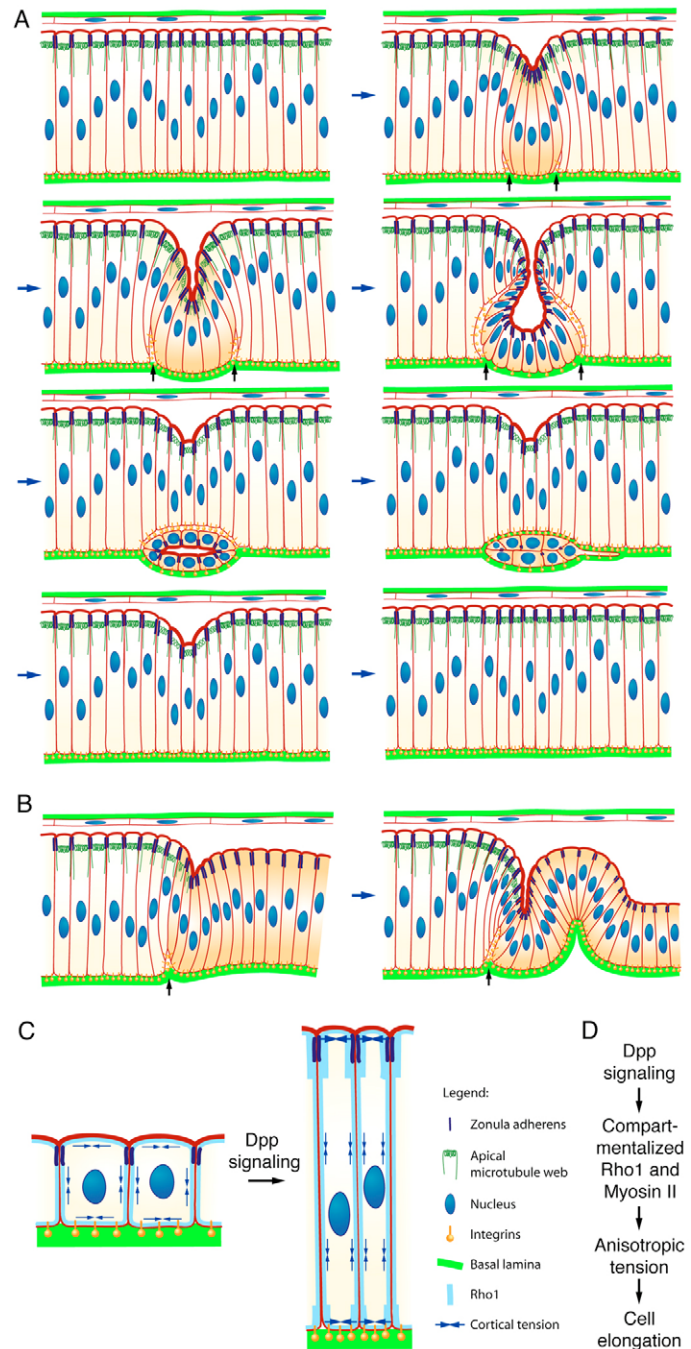


**Fig. 7.** Decreased Rho1 activity rescues the shortening of Dpp signaling compromised cells. (A-C) *x-z* sections of late third instar wing discs coexpressing Dad and p35 with Rho1<sup>N19</sup> (A), *sqh<sup>dsRNA</sup>* (B) or *Mbs<sup>N300</sup>* (C) in the dorsal compartment 52 hours after temperature shift to inducing conditions and stained as indicated. The apical-basal length of dorsal cells and control ventral cells is comparable (double-sided arrows). (D) The ratio of apical-basal length between dorsal and ventral cells of the experiments shown in A-C. Means  $\pm$  s.e.m. are depicted [ $n=14$  wing discs (control);  $n=3$  (*mbs<sup>N300</sup>, p35*);  $n=8$  (*GFP, dad, p35*);  $n=8$  (*Rho1<sup>N19</sup>, dad, p35*);  $n=6$  (*sqh<sup>dsRNA</sup>, dad, p35*);  $n=12$  (*mbs<sup>N300</sup>, dad, p35*)]; \* $P<0.001$ . Scale bars: 20  $\mu$ m.

**Fig. 8.** Dpp signaling and Rho1 in epithelial cell shape. (A) Schematic representation of the consequences of loss of Dpp signaling in *tkv<sup>Δ12</sup> bsk<sup>-</sup>* clones (dark brown) on epithelial morphology. *tkv<sup>Δ12</sup> bsk<sup>-</sup>* mutant cells initially constrict apicolaterally and shorten along their apical-basal axis, resulting in the formation of an apical epithelial invagination. At the same time, the basal epithelial surface indentates, juxtaposing the basal sides of mutant cells and neighboring wild-type cells. Subsequently, mutant cells lose junctional contact to neighboring cells and extrude from the basal side of the epithelium. Extruded cells form long actin-rich protrusions and are lost from the epithelium. The epithelium attains its normal shape. (B) Schematic representation of the consequences of a compartment-wide reduction in Dpp signaling on epithelial morphology. Schemes represent *ap-GAL4 tubP-gal80<sup>Δs</sup> UAS-dad UAS-p35* wing discs 48 hours (left) and 56 hours (right) after temperature shift to inducing conditions. Cells with reduced Dpp signaling are shown in dark brown. (C) Scheme depicting the role of Dpp signaling in the compartmentalization of Rho1 and apical-basal cell elongation. Blue arrows indicate cortical tension. Interpretative view of the localization of Rho1 (light blue). (D) The proposed mechanism controlling apical-basal cell length in wing discs. Black arrows in A and B indicate indentations of the basal epithelial surface. *x-z* views are shown.

boundaries of Dpp signaling at clone borders from cell-autonomous functions of Dpp signaling. They demonstrate that the cell-autonomous function of Dpp signaling is not to prevent apical cell constriction, folding and cell extrusion, but rather to maintain proper columnar cell shape. Moreover, three further observations suggest that Dpp signaling has an instructive role that drives cell elongation. First, in the wild type, an increase in Dpp signal transduction activity correlated with apical-basal cell elongation in second instar larval discs. Second, in wing discs of late third instar larvae, Dpp signal transduction activity correlated with apical-basal cell length along the anteroposterior axis. Third, activation of Dpp signaling, by expressing the constitutively active Dpp receptor *Tkv<sup>Q-D</sup>*, resulted



in precocious cell elongation and apical cell narrowing during early larval development. These findings indicate that Dpp signaling is an important trigger for the cuboidal-to-columnar transition in cell shape that occurs during mid-larval development.

#### Roles of Dpp signaling and Rho1 in promoting cell elongation

How does Dpp signaling promote the apical-basal elongation of wing disc cells? Compartmentalization of Rho1 activity has been recognized as being important for shaping cells and tissues (Bement et al., 2006; Simoes et al., 2006). In the wild-type wing disc, Rho1 protein is enriched and the activity of the Rho1 sensor is increased at the apicolateral side, and more moderately at the basal side, of elongated cells. By contrast, Rho1 activity is more uniform in cuboidal cells, and overexpression of RhoGEF2, which leads to uniform distribution of this protein (Fig. 6D) and presumably also uniform Rho1 activity, resulted in a cuboidal cell shape. Rho1, when present at the apicolateral side of cells, might therefore have a function in stabilizing or promoting cell elongation. Since the apicolateral increase in Rho1 sensor activity correlated with an increase of P-MRLC at a similar location (compare Fig. 1L and Fig. 4F), this function of Rho1 might be mediated by myosin II. Our observation that a decrease in the bulk of Rho1 activity, either through expression of Rho1<sup>N19</sup> or *rho1<sup>dsRNA</sup>*, resulted in cell elongation rather than in cell shortening, further suggests that the compartmentalization of Rho1 activity is important for shaping wing disc cells. Future studies will need to examine the morphogenetic consequences of locally modulating the activity of Rho1.

Our results provide strong evidence for a functional link between Dpp signaling and Rho1-myosin II. We have shown that the shortening of cells with compromised Dpp signaling could be rescued by a decrease in Rho1 or MRLC activity. In particular, the expression of Mbs<sup>N300</sup>, an activated form of a subunit of myosin light chain phosphatase, which in wild-type wing discs did not significantly alter cell length, did rescue the shortening of Dpp-compromised cells (Fig. 7). This indicates a specific interaction between Dpp signaling and Mbs-myosin II. Our data further suggest that Dpp signaling controls apical-basal cell length by compartmentalizing Rho1 protein abundance and/or activity. First, in late third instar wing discs, apicolateral enrichment of Rho1 protein and Rho1 sensor activity directly correlated with the local level of Dpp signal transduction activity. Second, Rho1 protein abundance and Rho1 sensor activity were decreased at the apicolateral side of cells when Dpp signal transduction was compromised by expression of Dad. Third, Rho1 protein and Rho1 sensor activity were increased at the apicolateral side and also at the basal side of cells when Dpp signal transduction was activated during early development by expression of Tkv<sup>Q-D</sup>.

Local activation of Rho1 and myosin II can lead to contraction of actin-myosin filaments, which can increase the cortical tension that is important for the shaping of cells during various developmental processes (reviewed by Lecuit and Lenne, 2007). By compartmentalizing Rho1 activity, Dpp signaling might promote both apical-basal cell elongation and apical cell narrowing. An increase in tension at the apicolateral cell cortex might promote apical cell narrowing. At the same time, a relative decrease in cortical tension laterally, compared with that on the apicolateral side, might allow cells to elongate through intrinsic cytoskeletal forces and/or extrinsic forces imposed by the growth of the epithelium. In this model (Fig. 8C,D), Dpp signaling directs the cuboidal-to-columnar shape transition of wing disc cells by increasing the Rho1 and myosin II activities at the apicolateral side of cells. The local

increase of Rho1 and myosin II activities might then shift the balance of tension between the apicolateral cell cortex and the lateral cell cortex towards an increased tension at the apicolateral cell cortex.

Our results identify a Dpp-Brk-Rho1-myosin II pathway controlling cell shape in the wing disc epithelium. The elimination of Brk function in *mad<sup>-</sup>* mutant cells allowed these cells to maintain a normal columnar cell shape (Fig. 2J,K), indicating that Dpp controls epithelial morphogenesis through repression of Brk. Since Brk acts as a transcriptional repressor, the link between Brk and Rho1 is most probably established through an unknown Brk-repressible gene. The identification of genes transcriptionally repressed by Brk will thus be important for determination of how Dpp signaling controls Rho1 and thereby, epithelial cell shape. Our finding that Dpp signaling has a cell-autonomous morphogenetic function indicates that Dpp signaling provides a connection between cell-fate specification, cell growth and the control of morphogenesis. It, thereby, might help to facilitate the coordination of these processes during wing disc development.

Given the evolutionary conserved functions of Rho and myosin II, we anticipate that the mechanisms regulating columnar cell shape, which we describe here for the wing disc, will also operate in a wide range of other epithelia. Moreover, the role of TGFβ/Dpp signaling in patterned morphogenesis appears to be conserved in vertebrates (Gibson and Perrimon, 2005), raising the possibility that Rho and myosin II are common mediators of TGFβ/Dpp signaling.

## Materials and Methods

### *Drosophila* stocks

The following fly stocks were used: *tkv<sup>Δ12</sup>*, *Df(2L)flp147E*, a deficiency removing *bsk*, *mbs<sup>T666</sup>*, *brk-lacZ*, *Act5C>CD2>GAL4*, *ap-GAL4*, *nub-GAL4*, *tubP-gal80<sup>F</sup>*, *UAS-dad*, *UAS-p35*, *UAS-CDS-GFP*, *UAS-Rho1<sup>N19</sup>*, *UAS-Rho1<sup>V14</sup>*, *UAS-RhoGEF2*, *UAS-sqh<sup>E20E21</sup>*, *UAS-moesin<sup>dsRNA327-775</sup>*, *UAS-mbs<sup>N300</sup>*, *UAS-tkv*, *UAS-tkv<sup>Q-D</sup>*, *UAS-tkv<sup>DGSK</sup>*, *UAS-PKNG58AeGFP* and *viking-GFP* (see Flybase (<http://flybase.bio.indiana.edu>) for description). *UAS-Rho1<sup>dsRNA</sup>*, *UAS-sqh<sup>dsRNA</sup>* and *UAS-dia<sup>dsRNA</sup>* were from the Vienna Drosophila RNAi Center, #12734, #7917 and #20518, respectively (Dietzl et al., 2007). *brk<sup>ΔH</sup> mad<sup>-</sup>* clones were as previously described (Shen and Dahmann, 2005b).

Marked clones were generated by Flp-mediated mitotic recombination (Lee and Luo, 1999; Xu and Rubin, 1993) subjecting larvae to a 35–38.5°C heat shock for 30 minutes. Transgenes were expressed using the GAL4-UAS system (Brand and Perrimon, 1993). To control timing of transgene expression using TARGET (McGuire et al., 2003), larvae raised at 18°C were shifted for the indicated time to 29°C before analysis.

### Molecular cloning

To generate *UAS-kat60* and *UAS-Klp10A*, coding sequences were PCR-amplified from ESTs RE17942 and LD29208, respectively. Primers were 5'-GGGGTACCTA-CAAACACAGGCAGGCAGCAG-3' and 5'-GCTCTAGACAGAGGGAAC-TTCTGGTACAC-3' for *kat60* and GGGGTACCGTAGCGGTTGGGAA-GATAGCAG-3' and 5'-GCTCTAGAGTAGATTTGTGCCGTGGCATGAAC-3' for *Klp10A*. Restriction sites for cloning into pUAST are underlined.

### Immunohistochemistry

Discs were fixed and stained according to standard protocols. Wing discs, except in Fig. 1F–H, Fig. 2A–C, Fig. 5A–G, supplementary material Fig. S1D–G and Fig. S3, were mounted using double-sided tape (Tesa 05338, Beiersdorf, Hamburg) with the apical side of the columnar epithelium facing the coverslip, except in Fig. 2E–I, Fig. 3D, supplementary material Fig. S1A–C,G–O, Fig. S2A–D and Fig. S5C–F, where the basal side faced the coverslip to allow better visualization of basal cell structures. Primary antibodies used were mouse anti-GFP, 1:100 (Santa Cruz), rabbit anti-GFP, 1:2000 (Clontech), rabbit anti-β-Gal, 1:2000 (Cappel), mouse anti-β-Gal, 1:2000 (Promega), rat anti-DE-cadherin (DCAD2), 1:50 (Oda et al., 1994), rabbit anti-phospho-Ser19-MRLC, 1:10 (Cell Signaling Technology), mouse anti-α-tubulin, 1:200 (Sigma), mouse anti-FasIII, 1:200 (Developmental Studies Hybridoma Bank, DSHB), rabbit anti-Moesin, 1:50 (Edwards et al., 1997), mouse anti-Dlg, 1:200 (DSHB), rabbit anti-p35, 1:500 (Biocarta), mouse anti-Rho1, 1:100 (DSHB), rabbit anti-RhoGEF2, 1:50 (Grosshans et al., 2005), rabbit anti-Dia, 1:400 (Afshar et al., 2000), rabbit anti-Pmad, 1:50 (Persson et al., 1998), mouse anti-PSβ-integrin, 1:10 (DSHB), mouse anti-Wingless, 1:100 (DSHB), rat anti-Crb, 1:100 (Richard et al., 2006), rabbit anti-Spalt, 1:30 (gift from Reinhard Schuh, Max-Planck-Institut für

Biophysikalische Chemie, Göttingen, Germany) and rabbit anti-Twist (1:100) (Thisse et al., 1988). Secondary antibodies (Molecular Probes), all diluted 1:200, were anti-mouse Alexa Fluor 488, anti-rabbit Alexa Fluor 488, anti-mouse Alexa Fluor 555, anti-mouse Cy5, anti-rat Cy5 and anti-rabbit Cy5. Rhodamine-phalloidin and DAPI (both Molecular Probes) were diluted 1:200 and 1:500, respectively. To compare Rho sensor activity, control and experimental wing discs were stained in parallel, mounted on the same microscope slide and imaged with identical settings on the microscope. Images were recorded on a LSM510 Zeiss confocal microscope. 3D renderings were made using Volocity.

### Measurements

The plot shown in Fig. 1K was generated by first discretizing into 82 bins the entire basal surface of the wing disc as displayed in Fig. 1J. For each bin, the orthogonal distance from the basal surface to the apical surface of the columnar epithelium was determined. The mean pixel intensity of the *brk-lacZ* staining was measured in an 18- $\mu\text{m}$ -wide strip centering on the nuclei. Background pixel intensity, as measured in the area outside the nuclei, was subtracted. In Fig. 5J, the mean apical pixel intensity was measured in a 3.5- $\mu\text{m}$ -wide strip below the apical surface of the epithelium. The lateral pixel intensity was determined in a strip corresponding to the apical-basal position of the nuclei. Pixel intensities were measured using ImageJ. For determining the relative apical-basal length of cells, confocal images showing cross-sectional views of wing discs (see for example, Fig. 3A) were printed and the distance between the apical and basal surfaces of the columnar epithelium in the middle of the ventral wing disc pouch and in the middle of the dorsal wing disc pouch were measured using a ruler. The characteristic fold that is present between the hinge and the pouch (see Fig. 1E) was used to identify the wing disc pouch. For measuring relative cross section areas, regions of printouts showing the same number of cells for the dorsal and ventral compartments, as counted by DAPI-stained nuclei, were excised and weighed. Statistical analysis was performed using a Welch's *t*-test.

We thank Heather M. Thompson (Max Planck Institute of Molecular Cell Biology and Genetics, Dresden, Germany) for providing the data shown in Fig. 1F-H; J.-Y. Tinevez for assistance with the image analysis shown in Fig. 1K. We also thank K. Basler, S. Eaton, A. Garcia-Bellido, U. Häcker, A. Jacinto, M. Mlodzik, H. Oda, F. Pichaud, J. Treisman, T. Xu, the Bloomington *Drosophila* Stock Center and the Vienna *Drosophila* RNAi Center for fly stocks; J. Grosshans, D. Kiehart, E. Knust, F. Perrin-Schmitt, R. Schuh, P. ten Dijke and the Developmental Studies Hybridoma Bank for antibodies; and S. Eaton, C.-P. Heisenberg and E. Knust for critical comments on the manuscript. This work was supported by the Max Planck Society.

### References

- Adachi-Yamada, T. and O'Connor, M. B. (2002). Morphogenetic apoptosis: a mechanism for correcting discontinuities in morphogen gradients. *Dev. Biol.* **251**, 74-90.
- Adachi-Yamada, T., Fujimura-Kamada, K., Nishida, Y. and Matsumoto, K. (1999). Distortion of proximal-distal information causes JNK-dependent apoptosis in *Drosophila* wing. *Nature* **400**, 166-169.
- Affolter, M. and Basler, K. (2007). The Decapentaplegic morphogen gradient: from pattern formation to growth regulation. *Nat. Rev. Genet.* **8**, 663-674.
- Afshar, K., Stuart, B. and Wasserman, S. A. (2000). Functional analysis of the *Drosophila* diaphanous FH protein in early embryonic development. *Development* **127**, 1887-1897.
- Alessi, D., MacDougall, L. K., Sola, M. M., Ikebe, M. and Cohen, P. (1992). The control of protein phosphatase-1 by targeting subunits: the major myosin phosphatase in avian smooth muscle is a novel form of protein phosphatase-1. *Eur. J. Biochem.* **210**, 1023-1035.
- Amano, M., Ito, M., Kimura, K., Fukata, Y., Chihara, K., Nakano, T., Matsuura, Y. and Kaibuchi, K. (1996). Phosphorylation and activation of myosin by Rho-associated kinase (Rho-kinase). *J. Biol. Chem.* **271**, 20246-20249.
- Auerbach, C. (1936). The development of legs, wings, and halteres in wild type and some mutant strains of *Drosophila melanogaster*. *Trans. R. Soc. Edinb.* **58**, 787-815.
- Azpiazu, N. and Morata, G. (2000). Function and regulation of homothorax in the wing imaginal disc of *Drosophila*. *Development* **127**, 2685-2693.
- Barrett, K., Leptin, M. and Settleman, J. (1997). The Rho GTPase and a putative RhoGEF mediate a signaling pathway for the cell shape changes in *Drosophila* gastrulation. *Cell* **91**, 905-915.
- Bement, W. M., Miller, A. L. and von Dassow, G. (2006). Rho GTPase activity zones and transient contractile arrays. *BioEssays* **28**, 983-993.
- Bertet, C., Sulak, L. and Lecuit, T. (2004). Myosin-dependent junction remodelling controls planar cell intercalation and axis elongation. *Nature* **429**, 667-671.
- Brand, A. H. and Perrimon, N. (1993). Targeted gene expression as a means of altering cell fates and generating dominant phenotypes. *Development* **118**, 401-415.
- Brodu, V. and Casanova, J. (2006). The RhoGAP crossveinless-c links tracheal and EGFR signaling to cell shape remodeling in *Drosophila* tracheal invagination. *Genes Dev.* **20**, 1817-1828.
- Burke, R. and Basler, K. (1996). Dpp receptors are autonomously required for cell proliferation in the entire developing *Drosophila* wing. *Development* **122**, 2261-2269.
- Campbell, G. and Tomlinson, A. (1999). Transducing the Dpp morphogen gradient in the wing of *Drosophila*: regulation of Dpp targets by brinker. *Cell* **96**, 553-562.
- Cohen, S. M. (1993). Imaginal disc development. In *The Development of Drosophila Melanogaster* (ed. M. Bate and A. Martinez Arias), pp. 747-841. Cold Spring Harbor, NY: Cold Spring Harbor Laboratory Press.
- Corrigan, D., Walther, R. F., Rodriguez, L., Fichelson, P. and Pichaud, F. (2007). Hedgehog signaling is a principal inducer of Myosin-II-driven cell ingression in *Drosophila* epithelia. *Dev. Cell* **13**, 730-742.
- Craig, R., Smith, R. and Kendrick-Jones, J. (1983). Light-chain phosphorylation controls the conformation of vertebrate non-muscle and smooth muscle myosin molecules. *Nature* **302**, 436-439.
- Dawes-Hoang, R. E., Parmar, K. M., Christiansen, A. E., Phelps, C. B., Brand, A. H. and Wieschaus, E. F. (2005). folded gastrulation, cell shape change and the control of myosin localization. *Development* **132**, 4165-4178.
- Dietzl, G., Chen, D., Schnorrer, F., Su, K. C., Barinova, Y., Fellner, M., Gasser, B., Kinsey, K., Oppel, S., Scheiblauer, S. et al. (2007). A genome-wide transgenic RNAi library for conditional gene inactivation in *Drosophila*. *Nature* **448**, 151-156.
- Eaton, S., Wepf, R. and Simons, K. (1996). Roles for Rac1 and Cdc42 in planar polarization and hair outgrowth in the wing of *Drosophila*. *J. Cell Biol.* **135**, 1277-1289.
- Edwards, K. A., Demsky, M., Montague, R. A., Weymouth, N. and Kiehart, D. P. (1997). GFP-moesin illuminates actin cytoskeleton dynamics in living tissue and demonstrates cell shape changes during morphogenesis in *Drosophila*. *Dev. Biol.* **191**, 103-117.
- Entchev, E. V., Schwabedissen, A. and Gonzalez-Gaitan, M. (2000). Gradient formation of the TGF-beta homolog Dpp. *Cell* **103**, 981-991.
- Escudero, L. M., Bischoff, M. and Freeman, M. (2007). Myosin II regulates complex cellular arrangement and epithelial architecture in *Drosophila*. *Dev. Cell* **13**, 717-729.
- Fox, D. T. and Peifer, M. (2007). Abelson kinase (Abl) and RhoGEF2 regulate actin organization during cell constriction in *Drosophila*. *Development* **134**, 567-578.
- Fristrom, D. and Fristrom, J. W. (1993). The metamorphic development of the adult epidermis. In *The Development of Drosophila Melanogaster* (ed. M. Bate and A. Martinez Arias), pp. 843-897. Cold Spring Harbor, NY: Cold Spring Harbor Laboratory Press.
- Fristrom, D., Wilcox, M. and Fristrom, J. (1993). The distribution of PS integrins, laminin A and F-actin during key stages in *Drosophila* wing development. *Development* **117**, 509-523.
- Gibson, M. C. and Perrimon, N. (2005). Extrusion and death of DPP/BMP-compromised epithelial cells in the developing *Drosophila* wing. *Science* **307**, 1785-1789.
- Goshima, G. and Vale, R. D. (2003). The roles of microtubule-based motor proteins in mitosis: comprehensive RNAi analysis in the *Drosophila* S2 cell line. *J. Cell Biol.* **162**, 1003-1016.
- Grosshans, J., Wenzl, C., Herz, H. M., Bartoszewski, S., Schnorrer, F., Vogt, N., Schwarz, H. and Muller, H. A. (2005). RhoGEF2 and the formin Dia control the formation of the furrow canal by directed actin assembly during *Drosophila* cellularisation. *Development* **132**, 1009-1020.
- Hacker, U. and Perrimon, N. (1998). DRhoGEF2 encodes a member of the Dbl family of oncogenes and controls cell shape changes during gastrulation in *Drosophila*. *Genes Dev.* **12**, 274-284.
- Haerry, T. E., Khalsa, O., O'Connor, M. B. and Wharton, K. A. (1998). Synergistic signaling by two BMP ligands through the SAX and TKV receptors controls wing growth and patterning in *Drosophila*. *Development* **125**, 3977-3987.
- Hartshorne, D. J., Ito, M. and Erdodi, F. (1998). Myosin light chain phosphatase: subunit composition, interactions and regulation. *J. Muscle Res. Cell Motil.* **19**, 325-341.
- Hay, B. A., Wolff, T. and Rubin, G. M. (1994). Expression of baculovirus P35 prevents cell death in *Drosophila*. *Development* **120**, 2121-2129.
- Jaffe, A. B. and Hall, A. (2005). Rho GTPases: biochemistry and biology. *Annu. Rev. Cell Dev. Biol.* **21**, 247-269.
- Jazwinska, A., Kirov, N., Wieschaus, E., Roth, S. and Rushlow, C. (1999). The *Drosophila* gene *brinker* reveals a novel mechanism of Dpp target gene regulation. *Cell* **96**, 563-573.
- Knust, E. and Bossinger, O. (2002). Composition and formation of intercellular junctions in epithelial cells. *Science* **298**, 1955-1959.
- Kolsch, V., Seher, T., Fernandez-Ballester, G. J., Serrano, L. and Leptin, M. (2007). Control of *Drosophila* gastrulation by apical localization of adherens junctions and RhoGEF2. *Science* **315**, 384-386.
- Lecuit, T. and Lenne, P. F. (2007). Cell surface mechanics and the control of cell shape, tissue patterns and morphogenesis. *Nat. Rev. Mol. Cell Biol.* **8**, 633-644.
- Lecuit, T., Brook, W. J., Ng, M., Calleja, M., Sun, H. and Cohen, S. M. (1996). Two distinct mechanisms for long-range patterning by Decapentaplegic in the *Drosophila* wing. *Nature* **381**, 387-393.
- Lee, A. and Treisman, J. E. (2004). Excessive Myosin activity in *mbs* mutants causes photoreceptor movement out of the *Drosophila* eye disc epithelium. *Mol. Biol. Cell* **15**, 3285-3295.
- Lee, T. and Luo, L. (1999). Mosaic analysis with a repressible cell marker for studies of gene function in neuronal morphogenesis. *Neuron* **22**, 451-461.
- Lee, T., Winter, C., Marticic, S. S., Lee, A. and Luo, L. (2000). Essential roles of *Drosophila* RhoA in the regulation of neuroblast proliferation and dendritic but not axonal morphogenesis. *Neuron* **25**, 307-316.
- Leptin, M. (2005). Gastrulation movements: the logic and the nuts and bolts. *Dev. Cell* **8**, 305-320.
- Li, W. and Baker, N. E. (2007). Engulfment is required for cell competition. *Cell* **129**, 1215-1225.
- Martin-Castellanos, C. and Edgar, B. A. (2002). A characterization of the effects of Dpp signaling on cell growth and proliferation in the *Drosophila* wing. *Development* **129**, 1003-1013.

- McClure, K. D. and Schubiger, G. (2005). Developmental analysis and squamous morphogenesis of the peripodial epithelium in *Drosophila* imaginal discs. *Development* **132**, 5033-5042.
- McGuire, S. E., Le, P. T., Osborn, A. J., Matsumoto, K. and Davis, R. L. (2003). Spatiotemporal rescue of memory dysfunction in *Drosophila*. *Science* **302**, 1765-1768.
- McNally, F. J. and Vale, R. D. (1993). Identification of katanin, an ATPase that severs and disassembles stable microtubules. *Cell* **75**, 419-429.
- Minami, M., Kinoshita, N., Kamoshida, Y., Tanimoto, H. and Tabata, T. (1999). brinker is a target of Dpp in *Drosophila* that negatively regulates Dpp-dependent genes. *Nature* **398**, 242-246.
- Mitonaka, T., Muramatsu, Y., Sugiyama, S., Mizuno, T. and Nishida, Y. (2007). Essential roles of myosin phosphatase in the maintenance of epithelial cell integrity of *Drosophila* imaginal disc cells. *Dev. Biol.* **309**, 78-86.
- Moreno, E., Basler, K. and Morata, G. (2002). Cells compete for decapentaplegic survival factor to prevent apoptosis in *Drosophila* wing development. *Nature* **416**, 755-759.
- Nellen, D., Burke, R., Struhl, G. and Basler, K. (1996). Direct and long-range action of a DPP morphogen gradient. *Cell* **85**, 357-368.
- Nikolaidou, K. K. and Barrett, K. (2004). A Rho GTPase signaling pathway is used reiteratively in epithelial folding and potentially selects the outcome of Rho activation. *Curr. Biol.* **14**, 1822-1826.
- Oda, H., Uemura, T., Harada, Y., Iwai, Y. and Takeichi, M. (1994). A *Drosophila* homolog of cadherin associated with armadillo and essential for embryonic cell-cell adhesion. *Dev. Biol.* **165**, 716-726.
- Persson, U., Izumi, H., Souchevnytskyi, S., Itoh, S., Grimsby, S., Engstrom, U., Heldin, C. H., Funahashi, K. and ten Dijke, P. (1998). The L45 loop in type I receptors for TGF-beta family members is a critical determinant in specifying Smad isoform activation. *FEBS Lett.* **434**, 83-87.
- Polesello, C. and Payre, F. (2004). Small is beautiful: what flies tell us about ERM protein function in development. *Trends Cell Biol.* **14**, 294-302.
- Richard, M., Grawe, F. and Knust, E. (2006). DPATJ plays a role in retinal morphogenesis and protects against light-dependent degeneration of photoreceptor cells in the *Drosophila* eye. *Dev. Dyn.* **235**, 895-907.
- Ridley, A. J. (2006). Rho GTPases and actin dynamics in membrane protrusions and vesicle trafficking. *Trends Cell Biol.* **16**, 522-529.
- Rosenblatt, J., Raff, M. C. and Cramer, L. P. (2001). An epithelial cell destined for apoptosis signals its neighbors to extrude it by an actin- and myosin-dependent mechanism. *Curr. Biol.* **11**, 1847-1857.
- Shen, J. and Dahmann, C. (2005a). Extrusion of cells with inappropriate Dpp signaling from *Drosophila* wing disc epithelia. *Science* **307**, 1789-1790.
- Shen, J. and Dahmann, C. (2005b). The role of Dpp signaling in maintaining the *Drosophila* anteroposterior compartment boundary. *Dev. Biol.* **279**, 31-43.
- Simoes, S., Denholm, B., Azevedo, D., Sotillos, S., Martin, P., Skaer, H., Hombria, J. C. and Jacinto, A. (2006). Compartmentalisation of Rho regulators directs cell invagination during tissue morphogenesis. *Development* **133**, 4257-4267.
- Speck, O., Hughes, S. C., Noren, N. K., Kulikaukas, R. M. and Fehon, R. G. (2003). Moesin functions antagonistically to the Rho pathway to maintain epithelial integrity. *Nature* **421**, 83-87.
- Spencer, F. A., Hoffmann, F. M. and Gelbart, W. M. (1982). Decapentaplegic: a gene complex affecting morphogenesis in *Drosophila melanogaster*. *Cell* **28**, 451-461.
- Strutt, D. I., Weber, U. and Mlodzik, M. (1997). The role of RhoA in tissue polarity and Frizzled signalling. *Nature* **387**, 292-295.
- Tanimoto, H., Itoh, S., ten Dijke, P. and Tabata, T. (2000). Hedgehog creates a gradient of DPP activity in *Drosophila* wing imaginal discs. *Mol. Cell* **5**, 59-71.
- Teleman, A. A. and Cohen, S. M. (2000). Dpp gradient formation in the *Drosophila* wing imaginal disc. *Cell* **103**, 971-980.
- Thiery, J. P. and Sleeman, J. P. (2006). Complex networks orchestrate epithelial-mesenchymal transitions. *Nat. Rev. Mol. Cell Biol.* **7**, 131-142.
- Thisse, B., Stoetzel, C., Gorostiza-Thisse, C. and Perrin-Schmitt, F. (1988). Sequence of the *twist* gene and nuclear localization of its protein in endomesodermal cells of early *Drosophila* embryos. *EMBO J.* **7**, 2175-2183.
- Tsuneizumi, K., Nakayama, T., Kamoshida, Y., Kornberg, T. B., Christian, J. L. and Tabata, T. (1997). Daughters against dpp modulates dpp organizing activity in *Drosophila* wing development. *Nature* **389**, 627-631.
- Ursprung, H. (1972). The fine structure of imaginal disks. In *The Biology of Imaginal Disks* (ed. H. Ursprung and R. Nothinger), pp. 93-107. Berlin: Springer Verlag.
- Van Aelst, L. and Symons, M. (2002). Role of Rho family GTPases in epithelial morphogenesis. *Genes Dev.* **16**, 1032-1054.
- Vidal, M., Larson, D. E. and Cagan, R. L. (2006). Csk-deficient boundary cells are eliminated from normal *Drosophila* epithelia by exclusion, migration, and apoptosis. *Dev. Cell.* **10**, 33-44.
- Wei, L., Roberts, W., Wang, L., Yamada, M., Zhang, S., Zhao, Z., Rivkees, S. A., Schwartz, R. J. and Imanaka-Yoshida, K. (2001). Rho kinases play an obligatory role in vertebrate embryonic organogenesis. *Development* **128**, 2953-2962.
- Winter, C. G., Wang, B., Ballew, A., Royou, A., Karess, R., Axelrod, J. D. and Luo, L. (2001). *Drosophila* Rho-associated kinase (Drok) links Frizzled-mediated planar cell polarity signaling to the actin cytoskeleton. *Cell* **105**, 81-91.
- Woods, D. F., Wu, J. W. and Bryant, P. J. (1997). Localization of proteins to the apico-lateral junctions of *Drosophila* epithelia. *Dev. Genet.* **20**, 111-118.
- Xu, T. and Rubin, G. M. (1993). Analysis of genetic mosaics in developing and adult *Drosophila* tissues. *Development* **117**, 1223-1237.
- Zavadil, J. and Bottinger, E. P. (2005). TGF-beta and epithelial-to-mesenchymal transitions. *Oncogene* **24**, 5764-5774.
- Zecca, M., Basler, K. and Struhl, G. (1995). Sequential organizing activities of engrailed, hedgehog and decapentaplegic in the *Drosophila* wing. *Development* **121**, 2265-2278.